

Diagrammatic Simplification of Linearized Coupled Cluster Theory

Kevin Carter-Fenk*

(Dated: April 17, 2025)

Linearized Coupled Cluster Doubles (LinCCD) often provides near-singular energies in small-gap systems that exhibit static correlation. This has been attributed to the lack of quadratic \hat{T}_2^2 terms that typically balance out small energy denominators in the CCD amplitude equations. Herein, I show that exchange contributions to ring and crossed-ring contractions (not small denominators *per se*) cause the divergent behavior of LinCC(S)D approaches. Rather than omitting exchange terms, I recommend a regular and size-consistent method that retains only linear ladder diagrams. As LinCCD and configuration interaction doubles (CID) equations are isomorphic, this also implies that simplification (rather than quadratic extensions) of CID amplitude equations can lead to a size-consistent theory. Linearized ladder CCD (LinLCCD) is robust in statically-correlated systems and can be made $\mathcal{O}(n_{\text{occ}}^4 n_{\text{vir}}^2)$ with a hole-hole approximation. The relationship between LinLCCD and random-phase approximation sets the stage for the development of next-generation double-hybrid density functionals that can describe static correlation.

Coupled cluster (CC) theory with double substitutions (CCD) is the simplest form of CC that captures electron correlation.¹ There are a host of advantages to linearized CCD methods (LinCCD) over full CCD,^{2,3} including reductions in memory demands, ease of spin-adapting the LinCCD wave function (albeit there is no rigorous wave function in linearized CC approximations),⁴ and simpler physical interpretation of the equations. My research group is particularly interested in the Hermitian formulation that is offered by linearized CC methods, as this can be useful in developing excited-state theories.⁵ Hermitian approaches are also quite powerful in the sense that they satisfy the generalized Hellmann-Feynman theorem, permitting simpler evaluation of forces (whereas left-eigenvectors are required in non-Hermitian CC approaches).⁶

However, linearized CC approaches often encounter near singularities in small-gap systems, affecting the performance of LinCCD away from equilibrium.⁷ Small orbital-energy gaps are often a qualitative indicator of static correlation,⁸ where the near-singular behavior of LinCCD can be further understood as a deficiency resultant from the lack of quadratic \hat{T}_2^2 terms that fold in higher-order correlation effects necessary to describe static correlation. In other words, LinCCD lacks the implicit account for quadruple excitations that is found in the CCD amplitude equations, making it unable to counteract small energy denominators. Consequently, LinCCSD has been combined with Tikhonov regularization⁹ as a means of sidestepping divergences.⁷ Multireference LinCC approaches have also been developed to avoid divergences in systems that exhibit static correlation, albeit at increased cost.^{10–12}

Beyond LinCCD, there are classes of CC approaches that attempt to correct errors within single-reference CC that arise due to static correlation. These “addition-by-subtraction” (ABS) CC methods take the somewhat paradoxical approach of removing components of the \hat{T} operator that are found to be particularly ill-behaved in the face of static correlation.¹³ Perhaps the most well-known ABS-CC approach is pair CCD, where only

pair double substitution clusters are retained, leading to an approach that can describe single and double-bond dissociation.^{14–17} Alternatively, it is also possible to decouple the singlet- and triplet-paired amplitudes in CCD to achieve similarly well-behaved bond dissociation curves.^{18,19} Though, such singlet/triplet-pair couplings occur through a quadratic term in the CCD equations so the divergence of LinCCD must be attributable to other factors.

Another flavor of ABS-CC approach restricts the CCD equations to certain classes of diagrams. For instance, CCD with only ring diagrams is equivalent to the particle-hole random-phase approximation (ph-RPA)^{20–22} and is especially applicable in the case of the high-density homogeneous electron gas. Beyond single-reference approaches, diagrammatic re-summations of the ring diagrams have been recently applied to extend ph-RPA to the multireference case.²³

At the other end of the spectrum, CCD restricted to ladder diagrams (ladder-CCD) is formally equivalent to particle-particle RPA (pp-RPA)^{24,25} and is especially suitable in the limit of the low-density electron gas due to its explicit account of particle-particle correlations. Diagrammatic analysis of the ring and ladder CC equations has revealed that ring and ladder diagrams mainly describe long and short-ranged correlation effects, respectively.²⁶ These naturally imposed length scales have been leveraged in combinations of ladder- and ring-CCD via range-separation techniques, leading to promising methods for describing systems that do not exist in either extreme.²⁷

In this work, I present an ABS linearized CCD approach that linearizes the ladder CCD amplitude equations. By removing the terms associated with ring and crossed-ring diagrams from LinCCD, the resultant linearized ladder CCD (LinLCCD) approach avoids the near-singularities encountered in the former. Furthermore, the isomorphism between LinCCD and configuration interaction with double substitutions (CID) suggests that LinCCD equations are not size-consistent.¹ A lack of size-consistency implies that, for well-separated molec-

ular fragments A and B , $E_{A \cup B} = E_A + E_B$ is not satisfied by LinCCD/CID. While quadratic corrections have been added to CID to obtain CCD equations,^{28–33} revealing the role of \hat{T}_2^2 terms in size-consistent approaches, I propose that removing ring/crossed-ring terms from the LinCCD (or equivalently CID) equations as an alternative route to obtain a size-consistent, size-extensive, orbital invariant, and naturally regular method.

Throughout this work, I will denote occupied orbitals as i, j, k, l, \dots , virtual orbitals as a, b, c, d, \dots , and general unspecified orbitals as p, q, r, s, \dots . The abbreviations n_v and n_o will be used for the number of virtual orbitals and the number of occupied orbitals, respectively. Einstein summation notation is used except in limited cases where the summation is explicitly written out.

LinCCD invokes the approximation that the usual exponential parameterization of the wave function,

$$|\Psi_{\text{CC}}\rangle = e^{\hat{T}}|\Phi_{\text{HF}}\rangle \quad (1)$$

is Taylor-expanded through first order such that,

$$|\Psi_{\text{LinCC}}\rangle \approx (1 + \hat{T})|\Phi_{\text{HF}}\rangle. \quad (2)$$

By retaining only strongly-connected diagrams, the LinCCD energy can be cast in terms of a Hermitian Hamiltonian,

$$E = \langle \Phi_{\text{HF}} | [(1 + \hat{T}_2^\dagger) \hat{H} (1 + \hat{T}_2)]_{\text{SC}} | \Phi_{\text{HF}} \rangle \quad (3)$$

where,

$$\hat{T}_2 = \sum_{\substack{i>j \\ a>b}} t_{ij}^{ab} \hat{a}_a^\dagger \hat{a}_i^\dagger \hat{a}_b \hat{a}_j \quad (4)$$

is the usual double-substitution operator and the subscript SC indicates that only the strongly-connected diagrams are retained. The corresponding doubles amplitude equations are,

$$\begin{aligned} 0 = & v_{ij}^{ab} - \mathcal{P}_{ij}(t_{kj}^{ab} f_i^k) + \mathcal{P}_{ab}(f_c^a t_{ij}^{cb}) \\ & + \frac{1}{2} t_{kl}^{ab} v_{ij}^{kl} + \frac{1}{2} v_{cd}^{ab} t_{ij}^{cd} \\ & + \mathcal{P}_{ij} \mathcal{P}_{ab}(v_{ic}^{ak} t_{kj}^{cb}) \end{aligned} \quad (5)$$

where v_{pq}^{rs} are antisymmetrized 2-electron integrals $\langle rs || pq \rangle$ and $\mathcal{P}_{pq} = 1 - p \leftrightarrow q$ are index permutation operators. The first 3 terms (first line) of Eq. 5 are often referred to as the *driver* terms (the latter two of which are responsible for the energy denominator in perturbation theory). The fourth and fifth terms (middle line of Eq. 5) are associated with *ladder* diagrams, and the final term (last line) emerges from *ring* and *crossed-ring* diagrams. Finally, the LinCCD energy expression in the spatial-orbital basis is explicitly:

$$E = \frac{1}{4} v_{ab}^{ij} t_{ij}^{ab} \quad (6)$$

Interestingly, to my knowledge it has yet to be observed that retaining only *driver* terms and *ladder*-type

diagrams within LinCCD leads to naturally regular equations that are strongly resistant to divergence in molecular systems. Notably, linearized ladder approximations in various combinations with other RPA terms have been explored in the context of the homogeneous electron gas,^{34–38} but – to the best of my knowledge – were essentially abandoned before being applied in the context of chemistry. Given the tremendous volume of interest in pp-RPA/ladder-CCD approaches in quantum chemistry^{39–45} it appears pertinent to explore linearized ladder approximations.

Applying the same precedent of diagrammatic simplification as pp-RPA/ladder-CCD, I restrict LinCCD to ladder diagrams yielding,

$$\begin{aligned} 0 = & v_{ij}^{ab} + (f_c^a \delta_d^b + \delta_c^a f_d^b) t_{ij}^{cd} - (f_i^k \delta_j^l + \delta_i^k f_j^l) t_{kl}^{cd} \\ & + \frac{1}{2} t_{kl}^{ab} v_{ij}^{kl} + \frac{1}{2} v_{cd}^{ab} t_{ij}^{cd} \end{aligned} \quad (7)$$

These LinLCCD equations are naturally regular. In principle, the inclusion of only ladder diagrams incorporates the most important contributions for describing strong correlation. However, to understand precisely how this is the case, it is helpful to notice that the contractions in terms 2 and 4 and terms 3 and 5 can be grouped together,

$$\left(f_c^a \delta_d^b + \delta_c^a f_d^b + \frac{1}{2} v_{cd}^{ab} \right) t_{ij}^{cd} - \left(f_i^k \delta_j^l + \delta_i^k f_j^l - \frac{1}{2} v_{ij}^{kl} \right) t_{kl}^{cd} = -v_{ij}^{ab} \quad (8)$$

By choosing a clever basis for Eq. 8, such as the one that diagonalizes the $n_v^2 \times n_v^2$ matrix in term 1 and the $n_o^2 \times n_o^2$ matrix in term 2, the amplitude equation can be reduced to a highly revealing linear form,

$$(\tilde{\varepsilon}_a + \tilde{\varepsilon}_b - \tilde{\varepsilon}_i - \tilde{\varepsilon}_j) t_{ij}^{ab} = -\tilde{v}_{ij}^{ab} \quad (9)$$

where $\tilde{\varepsilon}_p$ and \tilde{v}_{ij}^{ab} are orbital energies and integrals in the dressed orbital basis, respectively. Such an isomorphism between second-order Møller-Plesset perturbation theory (MP2) and CCD equations has been noticed before, but only in the context of mosaic CCD.⁴⁶ In the linearized ladder context, the occupied and virtual orbital energies have been shifted by the hole-hole (hh) and particle-particle (pp) integrals, respectively. This essentially results in a set of screened first-order amplitudes wherein the energy gap is widened by adding hh correlations to the one-particle occupied pair energies and pp correlations to one-particle virtual pair energies, making LinLCCD robust against divergence in small-gap systems. Unlike mosaic CCD and myriad other renormalized MP2 theories,^{47–51} the LinLCCD gap is widened in an amplitude-independent way, suggesting that the LinLCCD equations could be solved non-iteratively, albeit such an approach would be quite impractical as it would require the diagonalization of a $n_v^2 \times n_v^2$ matrix.

Incredibly, removing the ring and crossed-ring contractions from LinCCD also corrects the size-consistency errors in the parent method. I note that beyond size-consistency, LinLCCD is also size-extensive and orbital

invariant. As the LinLCCD equations can be recast in the form of Eq. 9, the proof for size-consistency in this basis is trivial. Consider a system wherein molecules A and B are sufficiently far apart that their respective molecular orbitals may be trivially fragment-ascribed. After a rotation into the aforementioned dressed orbital basis Eq. 9 becomes zero for all sums over disjoint orbitals by means of the electron repulsion integrals, ensuring that the resultant energy satisfies $E_{A \cup B} = E_A + E_B$.

My group is particularly interested in low-scaling approximations that describe static correlation qualitatively well. While I will demonstrate the utility of LinLCCD, it does retain the most expensive $\mathcal{O}(n_o^2 n_v^4)$ particle-particle ladder term that is responsible for the $\mathcal{O}(N^6)$ cost of CCD. Evaluation of this term could be reduced to $\mathcal{O}(N^5)$ scaling using density fitting, or perhaps even further to $\mathcal{O}(N^4)$ with tensor hypercontraction.⁵² In the spirit of exploring low-scaling variants of linear ladder theories, I introduce one further approximation by completely removing the costly particle-particle ladder term to achieve,

$$\left(f_c^a \delta_d^b + \delta_c^a f_d^b\right) t_{ij}^{cd} - \left(f_i^k \delta_j^l + \delta_i^k f_j^l - \frac{1}{2} v_{ij}^{kl}\right) t_{kl}^{cd} = -v_{ij}^{ab} \quad (10)$$

thus shifting only the occupied-pair energies by the hole-hole ladder term. Unlike the LinLCCD case, there is no diagrammatic justification for removing the particle-particle ladder term, but the resultant LinLCCD(hh) approach is a potentially fruitful approximation that scales much more favorably as $\mathcal{O}(n_o^4 n_v^2)$.

I first show the relative robustness of LinLCCD methods through a few simple bond dissociation potential energy surfaces. The simplest case of H_2 in the STO-3G basis is shown in Fig. 1a. As expected, LinCCD diverges rapidly as the H-H bond is stretched. However, both LinLCCD and the further pruned LinLCCD(hh) approaches smoothly dissociate H_2 towards some limit, which is exact in the case of LinLCCD(hh). Of course, I note that these results also show that LinLCCD is no longer exact for all two electron systems, but neither is its (chemically very useful) parent ladder approximation, pp-RPA.

Interestingly, if the linear direct ring and crossed-ring terms (*i.e.* without antisymmetrizing the two-electron repulsion integrals) are retained alongside the fully antisymmetric ladder terms, the resultant LinLdRxRCCD approach also does not diverge. LinLdRxRCCD differs from full LinCCD only by the exchange component of the linear ring and crossed-ring contractions, implying that the term most responsible for the instability of LinCCD is not the small orbital-energy denominator *per se*, but the exchange ring/crossed-ring terms. In the case of HF molecule dissociation in Fig. 1b, this finding helps to explain why regularization by means of eliminating near-zero denominator terms in LinCCSD is only somewhat effective,⁷ eventually breaking down at large R_{H-F} , whereas LinLCCD, LinLCCD(hh), and LinLdRxRCCD are all stable out to 10^6 Å.

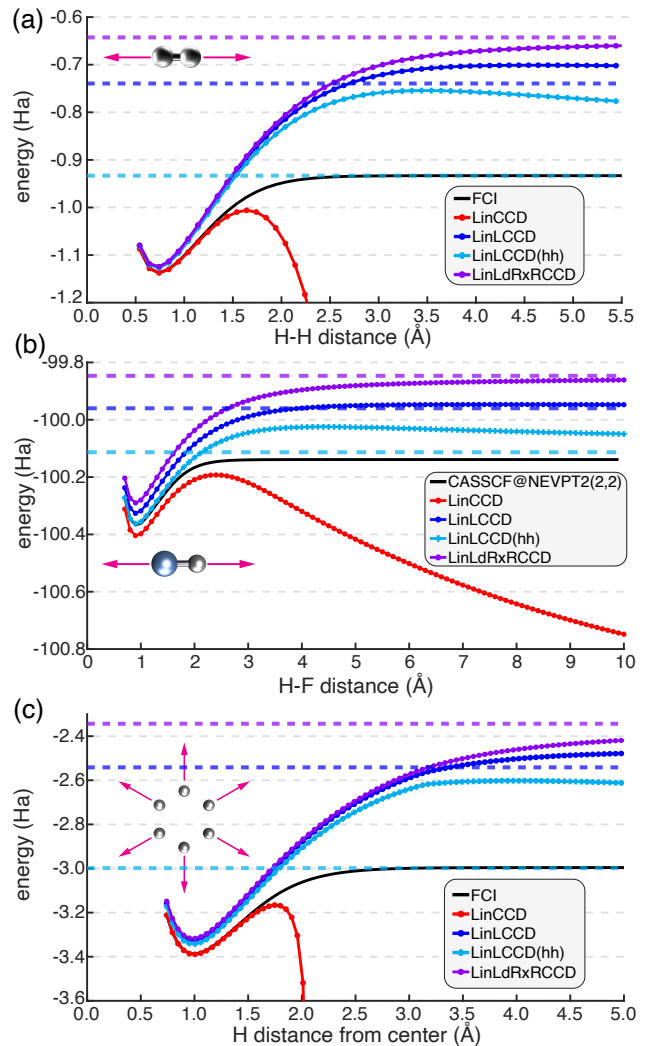


Figure 1. Dissociation curves for (a) hydrogen molecule in the minimal STO-3G basis set,⁵³ (b) Hydrogen fluoride molecule in the aug-cc-pVQZ basis,^{54,55} and (c) H_6 in the cc-pVDZ basis. Dashed lines of like-color indicate the dissociation limit for a particular method. Dissociation limits were estimated at $R = 10^6$ Å, except in the case of H_6 where $R = 10^3$ Å was used instead due to convergence difficulties.

I note that others have put forth that the divergence of CC equations alongside other deficiencies in statically-correlated systems manifest due to various exchange terms.^{20,25,56,57} Of course, removing exchange terms can lead to undesirable self-interaction artifacts, as is well known in the case of direct ring CCD (otherwise known as the direct ph-RPA), which over-binds significantly at equilibrium geometries.⁵⁸⁻⁶¹ Though less common, removing exchange terms from ladder CCD has also been explored but seems to lead to less satisfactory results for bond dissociation energies.⁶² Thus, if a self-interaction-free theory is desired that can smoothly dissociate bonds to a clear asymptotic limit, LinLCCD and LinLCCD(hh) represent suitable options.

Lastly in the series of bond dissociation curves, I inves-

tigate hexagonal H_6 dissociation in Fig. 1c. The hexagonal H_6 system is prototypical of strongly-correlated systems in chemistry and is reminiscent of the Hubbard model Hamiltonian. As the H_6 ring is expanded LinCCD rapidly diverges while all methods that exclude ring/crossed-ring exchange diagrams remain stable. The estimated asymptotic limit of LinLCCD(hh) appears somewhat deceptive as plotted because it very slightly overestimates the correlation energy at large R , dipping below the full configuration interaction (FCI) reference curve by about 4 mHa. While the LinLCCD(hh) potential curve is far too repulsive at intermediate R , the asymptotic limit remains very impressive for such an approximate scheme. Overall, all methods that remove the exchange ring/crossed-ring terms are robust for the bond stretching coordinates investigated in Fig. 1 while LinCCD fails in all cases, suggesting that ring/crossed-ring exchange contractions are to blame for the near-singular behavior of LinCCD.

Recall that LinLCCD is an approximation to pp-RPA, so it should not be expected to be a quantitatively accurate approach for total energies as pp-RPA – and therefore LinLCCD – does not offer ideal coverage of dynamical correlation effects.^{24,39,46} These deficiencies can be accounted for in pp-RPA by combination with density functionals, but I will not explore this here.^{41,43,63–66} The lack of dynamical correlation can be immediately seen in the potential energy curves of Fig. 1, as LinLCCD and LinLCCD(hh) both underestimate the magnitude of the correlation energy relative to FCI and LinCCD near equilibrium. However, much of the utility in RPA methods comes from how accurately they predict energy differences rather than the total energies themselves.²⁴ In this section I will explore the accuracy of LinLCCD for non-covalent interactions computed via,

$$\Delta E_{\text{int}} = E_{AB} - E_A - E_B, \quad (11)$$

where E_{AB} is the energy of the complex and E_X is the monomer energy of fragment X . All interaction energy calculations have been counterpoise corrected.⁶⁷

First, I examine the performance of LinLCCD, LinLCCD(hh), and LinCCD on the A24 data set of small dimers in Fig. 2a.⁶⁸ These results are largely unremarkable as all three methods perform statistically about the same with relatively low errors nearing just 0.1 kcal/mol in each case. Some notable differences are seen in Fig. 2b for the S22 data set which features several medium-sized π -stacked systems.^{69,70} Interestingly, while LinLCCD and LinLCCD(hh) perform similarly with quite low mean absolute errors (MAE) of 0.4 kcal/mol, LinCCD performs poorly with a MAE of 1.4 kcal/mol. The substantial degradation in performance of LinCCD on the S22 set is essentially due to π -stacked systems such as benzene dimer, pyrazine dimer, uracil dimer, indole...benzene, and adenine...thymine complexes for which all of the LinCCD errors exceed 1.5 kcal/mol. This overestimation of π -stacking interactions is mirrored by MP2, which is known to over-bind π -stacked complexes by upwards

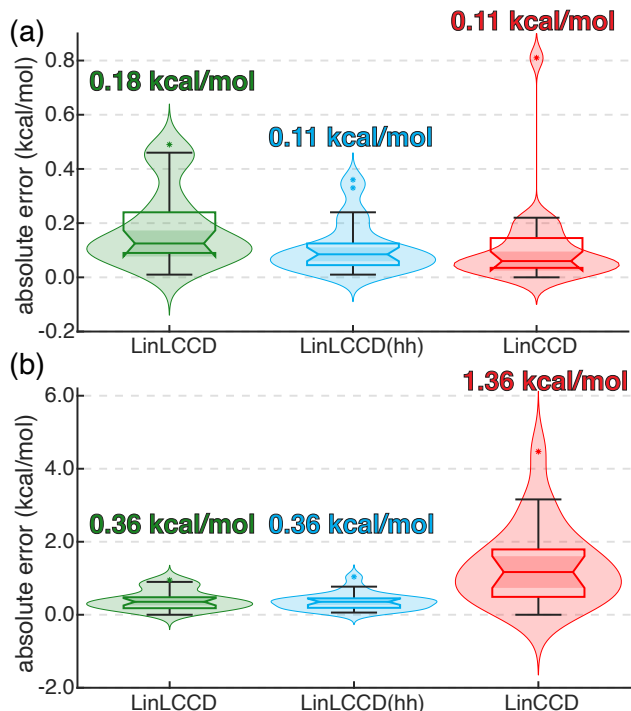


Figure 2. Error statistics for noncovalent interaction energies extrapolated to the complete basis set limit for (a) the A24 set of small dimers and (b) the S22 data set of small to medium sized dimers.

of 100%.^{71,72} The same over-binding is tempered substantially in LinLCCD, whose maximum error for the π -stacked subset is 0.85 kcal/mol. Both LinLCCD and LinLCCD(hh) methods appear to perform at least as well as regularized perturbation theory approaches.^{73,74} These results suggest that, despite a lack of dynamical correlation, the energy differences obtained with LinLCCD approaches can be reasonably accurate.

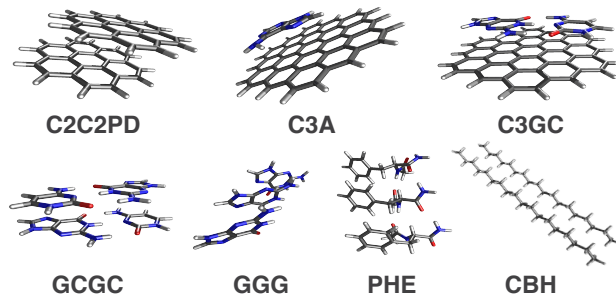


Figure 3. Systems that comprise the L7 data set along with their commonly employed acronyms.

In an effort to emphasize the relative affordability of the $\mathcal{O}(n_o^4 n_v^2)$ LinLCCD(hh) approximation, I also present complete basis set limit extrapolated interaction energies for the L7 data set of large dimers in Fig 3.⁷⁶ I compare to the complete basis set limit domain-localized pair natural

Table 1. Interaction Energies for L7 Data Set (kcal/mol)

System	LinLCCD(hh) ^a	BW-s2 ^{a,b}	MP2 ^{a,b}	CCSD(T ₀) ^{a,c}
C2C2PD	-34.54	-33.32	-38.08	-20.93 ± 0.44
C3A	-25.06	-24.11	-27.09	-17.49 ± 0.31
C3GC	-41.53	-40.40	-45.37	-29.24 ± 0.91
GCGC	-16.50	-17.00	-18.99	-13.54 ± 0.27
GGG	-3.31	-3.63	-4.54	-2.08 ± 0.09
CBH	-9.40	-10.90	-11.83	-11.00 ± 0.17
PHE	-25.94	-25.73	-26.32	-25.46 ± 0.01
MAE	5.36	4.78	7.18	—

^aExtrapolated to CBS limit.^bFrom Ref. 50.^cDLPNO-CCSD(T₀) from Ref. 75.

orbital (DLPNO)^{77–79} CCSD(T₀) benchmark data of Lao and co-workers.⁷⁵

The results in Table 1 show that MP2 dramatically overestimates the interaction energies in L7,⁷² which features several large π -stacked systems. As LinLCCD(hh) can be viewed as a renormalized MP2, it is of interest to contrast its performance with MP2 and with the renormalized MP2 approach known as size-consistent Brillouin-Wigner perturbation theory (BW-s2).⁷⁴ The results in Table 1 suggest that including hole-hole relaxation in the one-particle energies can temper the overestimated interaction energies of conventional MP2, but not dramatically so. The MAE is reduced relative to MP2 by nearly 2 kcal/mol, which is an improvement but suggests that linear ladder correlation is insufficient to achieve quantitative accuracy. The renormalization supplied by BW-s2 is somewhat more effective at suppressing over-correlation in the largest π -stacked systems than LinLCCD(hh), but less aggressive in systems like GCGC, GGG, and CBH, leading to an overall MAE that is about 0.6 kcal/mol lower than LinLCCD(hh). That said, the results between BW-s2 and LinLCCD(hh) are comparable to within 12% of one another. While I have shown that LinLCCD(hh) is affordable enough to be applied to such large systems and that the results are somewhat improved relative to MP2, some empiricism,⁵⁰ or other means of incorporating additional many-body screening effects could beget improvements.

Spin state energetics of transition metal complexes are a key quantity in the predictive modeling of energy relevant systems such as photoredox catalysts that are used to generate solar fuels such as H₂ and to facilitate organic syntheses.^{80–83} While there remains a paucity of benchmark-quality spin-state energetics data for transition metal complexes in the literature, the small Quest #8 data set of Loos and co-workers does provide excellent data for comparisons with non-relativistic quantum chemistry methods.^{84,85} The Quest #8 set contains 11 diatomic, monometallic transition metal molecules with non-relativistic theoretical best estimate (TBE) values computed in the gas phase, making comparison with other non-relativistic quantum chemistry methods more straightforward than (still useful) back-corrected experi-

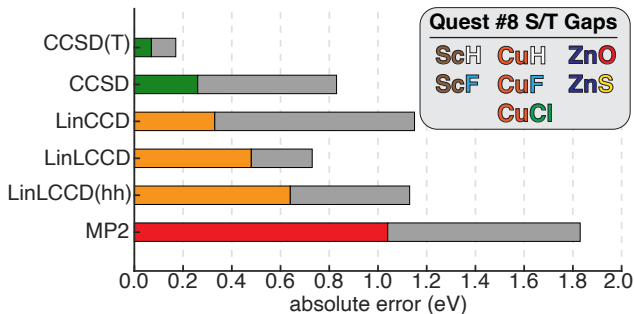


Figure 4. Mean absolute errors (shown as colored bars) and maximum errors (shown as gray bars) for the lowest energy singlet/triplet gaps in Quest #8 as computed by various Δ CC and Δ MP2 methods. The bars are colored according to the category of approximation being applied, where Møller-Plesset perturbation theory is red, linearized CC methods are orange, and nonlinear CC approaches are green. The systems in question are shown in the inset.

mental values.⁸⁶ Herein, I evaluate the performance of various correlated wave function theoretic approaches on the singlet/triplet gaps of the 7 molecule subset in Quest #8 that has a singlet ground state.

MAEs and maximum errors for the Quest #8 singlet/triplet gaps are shown in Fig. 4. None of the methods that truncate at double substitutions are quantitatively accurate relative to the TBE benchmarks, but the inclusion of perturbative triple excitations in CCSD(T) clearly has a large effect on the accuracy of the predicted gaps, reducing the MAE from 0.3 eV with CCSD to 0.07 eV with the inclusion of triples. As one might expect, LinCCD performs similarly well, albeit with a larger maximum error of 1.2 eV. Interestingly, while LinLCCD features a slightly larger MAE than LinCCD at 0.5 eV, it has a smaller maximum error than both LinCCD and CCSD at just 0.7 eV. Of all of the linearized CC approaches, LinLCCD(hh) performs the worst with a MAE of 0.6 eV, but it still outperforms MP2. As the linearized ladder CCD approaches can be conceptualized as intermediate theories between MP2 and LinCCD, it makes sense that their MAEs fall in a hierarchical order $MP2 > LinLCCD(hh) > LinLCCD > LinCCD$. While the results presented here are in line with expectations and are reasonably accurate, they once again point towards a need for incorporating more dynamical correlation into the LinLCCD approximation. Such studies are currently underway in my group.

The previous results focus mainly on energy differences between the electronic ground state and a high-spin triplet state of the system. This is one example of a Δ CC calculation, where the energy of each electronic configuration is optimized at the self-consistent field level and used as the reference for a subsequent non-Aufbau CC calculation. Excitation energies are then obtained by taking the difference between the CC energies of each respective calculation. In this section, I will explore the calculation of excited state bond dissociation curves via

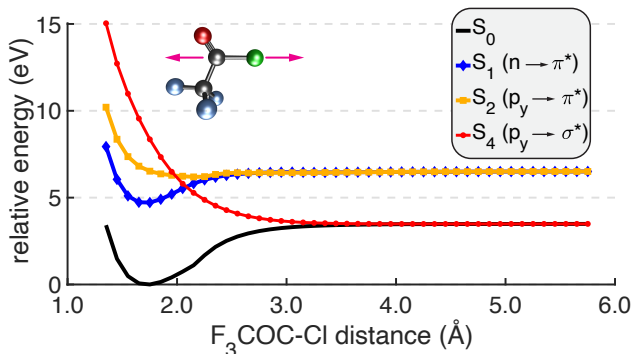


Figure 5. Dissociation of CF_3COCl along the C–Cl bond using $\Delta\text{LinLCCD}$ from reference configurations that represent the ground electronic state as well as $n \rightarrow \pi^*$, $p \rightarrow \pi^*$, and $p \rightarrow \sigma^*$ transitions.

the ΔCC approach to assess LinLCCD for its recovery of potential surfaces of open-shell systems.

Volatile organic compounds are of intense interest in the atmospheric chemistry community and understanding their photochemistry can inform on human health^{87,88} and global climate modeling.^{89–91} One downstream product of CHCl_2F , a common refrigerant, is CF_3COCl , which is known to decompose under UV irradiation.⁹² The results in Fig. 5 show $\Delta\text{LinLCCD}$ calculations on several of the lowest-energy excited states in CF_3COCl along the C–Cl bond stretching coordinate. Typically I would include single substitutions within the CC *ansatz* to model open-shell systems, but the presence of singles clusters threatens the stability of the excited-state configuration. By Thouless’ theorem,⁹³ single substitutions are equivalent to orbital rotations that could push the desired excited-state solutions towards the ground state. I note that methods such as Aufbau suppressed CC theory could be used to stabilize such singles-inclusive CC solutions.⁹⁴ Therefore, a caveat to bear in mind in the following analysis is that the reference determinant for each $\Delta\text{LinLCCD}$ excited state is spin contaminated and without single substitutions to aid in spin purification the calculated excitation energies are likely underestimated.^{95–97} While approximate spin projection could be employed,⁹⁸ I do not expect this to impact the qualitative validity of the results – especially for the purposes of modeling the topography of each potential surface at large C–Cl distances.

The dissociation curves for various states of CF_3COCl are shown in Fig. 5. All of the LinLCCD results are qualitatively consistent with the multireference calculations of Ref. 92. Namely, the S_1 state corresponds to a bound $n \rightarrow \pi^*$ transition at 4.7 eV, which is in good agreement with the experimental band maximum of about 4.9 eV.⁹² Furthermore, the S_2 and S_4 states are unbound and correspond to $p \rightarrow \pi^*$ and $p \rightarrow \sigma^*$ transitions, respectively. Both states lead to free dissociation to two different limits. This is expected, because dissociation along the ground state potential surface should lead to

the homolytic cleavage of the C–Cl σ bond, populating the σ^* orbital and resulting in the same dissociation limit as the S_4 state. In the case of the S_2 state, the occupied π^* orbital corresponds to a qualitatively different configuration at dissociation.

The dissociation limits for the ground state and S_2 states are 3.5 eV and 6.5 eV, respectively. The former is very close to the extended multistate complete active space second-order perturbation theory (XMS-CASPT2)⁹⁹ dissociation energy for S_0 predicted in Ref. 92 of 3.44 eV. The energy difference between S_0 and S_2 states at dissociation is 3 eV and is also in excellent agreement with XMS-CASPT2 results. Despite spin contamination, the qualitative curvature of each surface is reasonable and LinLCCD with open-shell singlet references provides excellent bond dissociation energies in the case of CF_3COCl .

In summary, I have introduced linearized ladder CCD equations alongside a linear hole-hole ladder approximation and examined their applicability to a range of chemistry contexts. LinLCCD and LinLCCD(hh) are both robust when static correlation becomes important, and LinLCCD(hh) serves as an affordable $\mathcal{O}(n_o^4 n_v^2)$ approximation that can be applied to large systems. I have also shown that the most problematic terms in LinCCD that lead to near-singular correlation energies are the ring and crossed-ring contractions – particularly the exchange contributions therein. It is particularly notable that LinLCCD is a size-consistent CID method that is obtained by removing linear terms rather than adding quadratic ones.²⁸ With future adaptations of LinLCCD and LinLCCD(hh) to incorporate more dynamical correlation, these approaches could prove to be quite useful in the design of new computational methodologies for modeling strongly correlated systems reasonably well within single-reference approximations.

Computational Details

All calculations were performed using a developer version of Q-Chem v6.2.¹⁰⁰ The A24 and S22 complete basis set limit results were obtained using two-point aug-cc-pVDZ/aug-cc-pVTZ extrapolation using $\beta = 2.51$ and $\alpha = 4.3$ as per Neese and Valeev.¹⁰¹ The S22 calculations made use of frozen natural orbitals (FNOs), retaining 99.6% of the natural orbital occupation.^{102–104} The use of FNOs has been shown to be a robust approximation that provides benchmark-quality non-covalent interaction energies on the S22 set.¹⁰⁵ The L7 calculations were extrapolated to the complete basis set limit using the somewhat smaller Def2-ma-SVP and Def2-ma-TZVP basis sets for heavy atoms and the corresponding Def2-SVP/Def2-TZVP for H atoms.^{106–108} As Neese and Valeev do not provide parameters to minimize extrapolation errors for Karlsruhe basis sets with diffuse functions,¹⁰¹ I computed the Hartree-Fock energies for L7 with the Def2-ma-QZVPP basis set and extrapolated the

correlation energy with the more typical $\beta = 3$ parameter. The L7 calculations are the only ones that use the frozen core approximation. The Quest#8 calculations employ the aug-cc-pVTZ basis for even-handed comparison with the aug-cc-pVTZ reference data in Ref. 85. Finally, the CF₃COCl potential energy surfaces were calculated using unrestricted Hartree-Fock reference orbitals. Non-Aufbau reference configurations were stabilized using a combination of state-targeted energy projection and initial maximum overlap method algorithms.^{109–111}

Acknowledgements

I thank Sylvia J. Bintrim and Abdulrahman Y. Zamani for our many engaging and enlightening discussions. This research was supported in part by the University of

Pittsburgh and the University of Pittsburgh Center for Research Computing, RRID:SCR_022735, through the resources provided. Specifically, this work used the H2P cluster, which is supported by NSF award number OAC-2117681.

Supporting Information

The Supporting Information is available free of charge at <https://pubs.acs.org/doi/10.1021/acs.jpcclett.XXXXXXX>

All A24 and S22 complete basis set limit data and Quest#8 data (XLSX)

-
- * Department of Chemistry, University of Pittsburgh, Pittsburgh, Pennsylvania 15218, USA; kay.carter-fenk@pitt.edu
- ¹ Szabo, A.; Ostlund, N. S. *Modern Quantum Chemistry*; Macmillan: New York, 1982.
 - ² Čížek, J. On the correlation problem in atomic and molecular systems. Calculation of wavefunction components in Ursell-type expansion using quantum-field theoretical methods. *J. Chem. Phys.* **1966**, *45*, 4256–4266.
 - ³ Bartlett, R. J. Many-body perturbation theory and coupled cluster theory for electron correlation in molecules. *Annu. Rev. Phys. Chem.* **1981**, *32*, 359–401.
 - ⁴ Li, X.; Paldus, J. A unitary group based open-shell coupled cluster study of vibrational frequencies in ground and excited states of first row diatomics. *J. Chem. Phys.* **1996**, *104*, 9555–9562.
 - ⁵ Bintrim, S. J.; Carter-Fenk, K. Optimal-reference excited state methods: Static correlation at polynomial cost with single-reference coupled-cluster approaches. *J. Chem. Theory Comput.* **2025**, .
 - ⁶ Crawford, T. D.; Schaefer III, H. F. An introduction to coupled cluster theory for computational chemists. In *Reviews in Computational Chemistry*, Vol. 14; Lipkowitz, K. B.; Boyd, D. B., Eds.; Wiley-VCH: New York, 2000; Chapter 2, pages 33–136.
 - ⁷ Taube, A. G.; Bartlett, R. J. Rethinking linearized coupled-cluster theory. *J. Chem. Phys.* **2009**, *130*, 144112:1–14.
 - ⁸ Hollet, J. W.; Gill, P. M. W. The two faces of static correlation. *J. Chem. Phys.* **2011**, *134*, 114111:1–5.
 - ⁹ Hansen, P. C. *Rank-deficient and discrete ill-posed problems: Numerical aspects of linear inversion, SIAM monographs on mathematical modeling and computation*; Society for Industrial and Applied Mathematics: Philadelphia, PA, 1998.
 - ¹⁰ Lyakh, D. I.; Musiał, M.; Lotrich, V. F.; Bartlett, R. J. Multireference nature of chemistry: The coupled-cluster view. *Chem. Rev.* **2012**, *112*, 182–243.
 - ¹¹ Sharma, S.; Alavi, A. Multireference linearized coupled cluster theory for strongly correlated systems using matrix product states. *J. Chem. Phys.* **2015**, *143*, 102815:1–9.
 - ¹² Jeanmairet, G.; Sharma, S.; Alavi, A. Stochastic multi-reference perturbation theory with application to the linearized coupled cluster method. *J. Chem. Phys.* **2017**, *146*, 044107:1–10.
 - ¹³ Bartlett, R. J. Perspective on Coupled-cluster Theory. The evolution toward simplicity in quantum chemistry. *Phys. Chem. Chem. Phys.* **2024**, *26*, 8013–8037.
 - ¹⁴ Stein, T.; Henderson, T. M.; Scuseria, G. E. Seniority zero pair coupled cluster doubles theory. *J. Chem. Phys.* **2014**, *140*, 214113:1–8.
 - ¹⁵ Henderson, T. M.; Bulik, I. W.; Stein, T.; Scuseria, G. E. Seniority-based coupled cluster theory. *J. Chem. Phys.* **2014**, *141*, 244104:1–10.
 - ¹⁶ Brzęk, F.; Boguslawski, K.; Tecmer, P.; Żuchowski, P. S. Benchmarking the accuracy of seniority-zero wave function methods for noncovalent interactions. *J. Chem. Theory Comput.* **2019**, *15*, 4021–4035.
 - ¹⁷ Boguslawski, K. Open-shell extensions to closed-shell pCCD. *Chem. Commun.* **2021**, *57*, 12277–12280.
 - ¹⁸ Bulik, I. W.; Henderson, T. M.; Scuseria, G. E. Can single-reference coupled cluster theory describe static correlation? *J. Chem. Theory Comput.* **2015**, *11*, 3171–3179.
 - ¹⁹ Gomez, J. A.; Henderson, T. M.; Scuseria, G. E. Recoupling the singlet- and triplet-pairing channels in single-reference coupled cluster theory. *J. Chem. Phys.* **2016**, *145*, 134103:1–7.
 - ²⁰ Scuseria, G. E.; Henderson, T. M.; Sorensen, D. C. The ground state correlation energy of the random phase approximation from a ring coupled cluster doubles approach. *J. Chem. Phys.* **2008**, *129*, 231101:1–4.
 - ²¹ Jansen, G.; Liu, R.-F.; Ángyán, J. G. On the equivalence of ring-coupled cluster and adiabatic connection fluctuation-dissipation theorem random phase approximation correlation energy expressions. *J. Chem. Phys.* **2010**, *133*, 154106:1–5.
 - ²² Chen, G. P.; Voora, V. K.; Agee, M. M.; Balasubramani, S. G.; Furche, F. Random-phase approximation methods. *Annu. Rev. Phys. Chem.* **2017**, *68*, 421–445.
 - ²³ Wang, Y.; Fang, W.-H.; Li, Z. Generalized many-body perturbation theory for the electron correlation energy: Multireference random phase approximation via diagram-

- matic resummation. *J. Phys. Chem. Lett.* **2025**, *16*, 3047–3055.
- ²⁴ Peng, D.; Steinmann, S. N.; Van Aggelen, H.; Yang, W. Equivalence of particle-particle random phase approximation correlation energy and ladder-coupled-cluster doubles. *J. Chem. Phys.* **2013**, *139*, 104112:1–8.
 - ²⁵ Scuseria, G. E.; Henderson, T. M.; Bulik, I. W. Particle-particle and quasiparticle random phase approximations: Connections to coupled cluster theory. *J. Chem. Phys.* **2013**, *139*, 104113:1–3.
 - ²⁶ Irmeler, A.; Gallo, A.; Hummel, F.; Grüneis, A. Duality of ring and ladder diagrams and its importance for many-electron perturbation theories. *Phys. Rev. Lett.* **2019**, *123*, 156401:1–6.
 - ²⁷ Shepherd, J. J.; Henderson, T. M.; Scuseria, G. E. Range-separated Brueckner coupled cluster doubles theory. *Phys. Rev. Lett.* **2014**, *112*, 133002:1–5.
 - ²⁸ Pople, J. A.; Head-Gordon, M.; Raghavachari, K. Quadratic configuration interaction. A general technique for determining electron correlation energies. *J. Chem. Phys.* **1987**, *87*, 5968–5975.
 - ²⁹ Cremer, D.; He, Z. Analysis of coupled cluster methods. IV. size-extensive quadratic CI methods – quadratic CI with triple and quadruple excitations. *Theoret. Chim. Acta* **1994**, *88*, 47–67.
 - ³⁰ Cremer, D.; He, Z. Size-extensive QCISDT – implementation and application. *Chem. Phys. Lett.* **1994**, *222*, 40–45.
 - ³¹ He, Z.; Kraka, E.; Cremer, D. Application of quadratic CI with singles, doubles, and triples (QCISDT): An attractive alternative to CCSDT. *Int. J. Quantum Chem.* **1996**, *57*, 157–172.
 - ³² He, Y.; He, Z.; Cremer, D. Size-extensive quadratic CI methods including quadruple excitations: QCISDTQ and QCISDTQ(6) – On the importance of four-electron correlation effects. *Chem. Phys. Lett.* **2000**, *317*, 535–544.
 - ³³ Cremer, D. From configuration interaction to coupled cluster theory: The quadratic configuration interaction approach. *WIREs Comput. Mol. Sci.* **2013**, *3*, 482–503.
 - ³⁴ Bishop, R. F.; Lüthmann, K. H. Electron correlations: I. Ground-state results in the high-density regime. *Phys. Rev. B* **1978**, *17*, 3757–3780.
 - ³⁵ Bishop, R. F.; Lüthmann, K. H. Electron correlations: II. Ground-state results at low and metallic densities. *Phys. Rev. B* **1982**, *26*, 5523–5557.
 - ³⁶ Freeman, D. L. Coupled-cluster summation of the particle-particle ladder diagrams for the two-dimensional electron gas. *J. Phys. C: Solid State Phys.* **1983**, *16*, 711–727.
 - ³⁷ Bishop, R. F.; Piechocki, W.; Stevens, G. A. Pairing correlations: I. The ground-state coupled-cluster formalism as a unifying approach. *Few-Body Systems* **1988**, *4*, 161–177.
 - ³⁸ Bishop, R. F.; Piechocki, W.; Stevens, G. A. Pairing correlations: II. Exact model ground-state results for generalised ladders. *Few-Body Systems* **1988**, *4*, 179–209.
 - ³⁹ Yang, Y.; Peng, D.; Davidson, E. R.; Yang, W. Singlet-triplet energy gaps for diradicals from particle-particle random phase approximation. *J. Phys. Chem. A* **2015**, *119*, 4923–4932.
 - ⁴⁰ Yang, Y.; Burke, K.; Yang, W. Accurate atomic quantum defects from particle-particle random phase approximation. *Mol. Phys.* **2015**, *114*, 1189–1198.
 - ⁴¹ Yang, Y.; Shen, L.; Zhang, D.; Yang, W. Conical Intersections from Particle-Particle Random Phase and Tamm-Dancoff Approximations. *J. Phys. Chem. Lett.* **2016**, *7*, 2407–2411.
 - ⁴² Yang, Y.; Dominguez, A.; Zhang, D.; Lutsker, V.; Niehaus, T. A.; Frauenheim, T.; Yang, W. Charge transfer excitations from particle-particle random phase approximation—Opportunities and challenges arising from two-electron deficient systems. *J. Chem. Phys.* **2017**, *146*, 124104:1–12.
 - ⁴³ Al-Saadon, R.; Sutton, C.; Yang, W. Accurate Treatment of Charge-Transfer Excitations and Thermally Activated Delayed Fluorescence Using the Particle-Particle Random Phase Approximation. *J. Chem. Theory Comput.* **2018**, *14*, 3196–3204.
 - ⁴⁴ Bannwarth, C.; Yu, J. K.; Hohenstein, E. G.; Martínez, T. J. Hole-hole Tamm-Dancoff-approximated density functional theory: A highly efficient electronic structure method incorporating dynamic and static correlation. *J. Chem. Phys.* **2020**, *153*, 024110:1–16.
 - ⁴⁵ Yu, J. K.; Bannwarth, C.; Hohenstein, E. G.; Martínez, T. J. *Ab initio* nonadiabatic molecular dynamics with hole-hole tamm-dancoff approximated density functional theory. *J. Chem. Theory Comput.* **2020**, *16*, 5499–5511.
 - ⁴⁶ Shepherd, J. J.; Henderson, T. M.; Scuseria, G. E. Coupled cluster channels in the homogeneous electron gas. *J. Chem. Phys.* **2014**, *140*, 124102:1–9.
 - ⁴⁷ Keller, E.; Tsatsoulis, T.; Reuter, K.; Margraf, J. T. Regularized second-order correlation methods for extended systems. *J. Chem. Phys.* **2022**, *156*, 024106:1–8.
 - ⁴⁸ Zhang, I. Y.; Rinke, P.; Scheffler, M. Wave-function inspired density functional applied to the H_2/H_2^+ challenge. *New J. Phys.* **2016**, *18*, 073026:1–16.
 - ⁴⁹ Zhang, I. Y.; Rinke, P.; Perdew, J. P.; Scheffler, M. Towards efficient orbital-dependent density functionals for weak and strong correlation. *Phys. Rev. Lett.* **2016**, *117*, 133002:1–5.
 - ⁵⁰ Carter-Fenk, K.; Shee, J.; Head-Gordon, M. Optimizing the regularization in size-consistent second-order Brillouin-Wigner perturbation theory. *J. Chem. Phys.* **2023**, *159*, 171104:1–8.
 - ⁵¹ Dittmer, L. B.; Head-Gordon, M. Repartitioning the Hamiltonian in many-body second-order Brillouin-Wigner perturbation theory: Uncovering new size-consistent models. *J. Chem. Phys.* **2025**, *162*, 054109:1–15.
 - ⁵² Shenvi, N.; van Aggelen, H.; Yang, Y.; Yang, W. Tensor hypercontracted ppRPA: Reducing the cost of the particle-particle random phase approximation from $\mathcal{O}(r^6)$ to $\mathcal{O}(r^4)$. *J. Chem. Phys.* **2014**, *141*, 024119:1–7.
 - ⁵³ Hehre, W. J.; Stewart, R. F.; Pople, J. A. Self-consistent molecular-orbital methods. I. Use of Gaussian expansions of Slater-type atomic orbitals. *J. Chem. Phys.* **1969**, *51*, 2657–2664.
 - ⁵⁴ Dunning, Jr., T. H. Gaussian basis sets for use in correlated molecular calculations. I. The atoms boron through neon and hydrogen. *J. Chem. Phys.* **1989**, *90*, 1007–1023.
 - ⁵⁵ Woon, D. E.; Dunning Jr., T. H. Gaussian basis sets for use in correlated molecular calculations. IV. Calculation of static electrical response properties. *J. Chem. Phys.* **1994**, *100*, 2975–2988.
 - ⁵⁶ Kats, D.; Manby, F. R. Communication: The distinguishable cluster approximation. *J. Chem. Phys.* **2013**, *139*.
 - ⁵⁷ Rishi, V.; Perera, A.; Bartlett, R. J. Assessing the distinguishable cluster approximation based on the triple bond-breaking in the nitrogen molecule. *J. Chem. Phys.* **2016**,

- 144.
- ⁵⁸ Mori-Sánchez, P.; Cohen, A. J.; Yang, W. Failure of the random-phase-approximation correlation energy. *Phys. Rev. A* **2012**, *85*, 042507:1–4.
 - ⁵⁹ Paier, J.; Ren, X.; Rinke, P.; Scuseria, G. E.; Grüneis, A.; Kresse, G.; Scheffler, M. Assessment of correlation energies based on the random-phase approximation. *New J. Phys.* **2012**, *14*, 043002:1–23.
 - ⁶⁰ Ruzsinszky, A.; Zhang, I. Y.; Scheffler, M. Insight into organic reactions from the direct random phase approximation and its corrections. *J. Chem. Phys.* **2015**, *143*, 144115:1–13.
 - ⁶¹ Ruan, S.; Ren, X.; Gould, T.; Ruzsinszky, A. Self-interaction-corrected random phase approximation. *J. Chem. Theory Comput.* **2021**, *17*, 2107–2115.
 - ⁶² Tahir, M. N.; Ren, X. Comparing particle-particle and particle-hole channels of the random phase approximation. *Phys. Rev. B* **2019**, *99*, 195149:1–12.
 - ⁶³ Van Aggelen, H.; Yang, Y.; Yang, W. Exchange-correlation energy from pairing matrix fluctuation and the particle-particle random-phase approximation. *Phys. Rev. A* **2013**, *88*, 030501:1–5.
 - ⁶⁴ Peng, D.; Van Aggelen, H.; Yang, Y.; Yang, W. Linear-response time-dependent density-functional theory with pairing fields. *J. Chem. Phys.* **2014**, *140*, 18A522:1–10.
 - ⁶⁵ Yang, Y.; Peng, D.; Lu, J.; Yang, W. Excitation energies from particle-particle random phase approximation: Davidson algorithm and benchmark studies. *J. Chem. Phys.* **2014**, *141*, 124104:1–10.
 - ⁶⁶ Jin, Y.; Yang, Y.; Zhang, D.; Peng, D.; Yang, W. Excitation energies from particle-particle random phase approximation with accurate optimized effective potentials. *J. Chem. Phys.* **2017**, *147*, 134105:1–7.
 - ⁶⁷ Boys, S. F.; Bernardi, F. The calculation of small molecular interactions by the differences of separated total energies. Some procedures with reduced errors. *Mol. Phys.* **1970**, *19*, 553–566.
 - ⁶⁸ Řezáč, J.; Hobza, P. Describing noncovalent interactions beyond the common approximations: How accurate is the “gold standard”, CCSD(T) at the complete basis set limit? *J. Chem. Theory Comput.* **2013**, *9*, 2151–2155.
 - ⁶⁹ Jurečka, P.; Šponer, J.; Černý, J.; Hobza, P. Benchmark database of accurate (MP2 and CCSD(T) complete basis set limit) interaction energies of small model complexes, DNA base pairs, and amino acid pairs. *Phys. Chem. Chem. Phys.* **2006**, *8*, 1985–1993.
 - ⁷⁰ Takatani, T.; Hohenstein, E. G.; Malagoli, M.; Marshall, M. S.; Sherrill, C. D. Basis set consistent revision of the S22 test set of noncovalent interaction energies. *J. Chem. Phys.* **2010**, *132*, 144104:1–5.
 - ⁷¹ Carter-Fenk, K.; Lao, K. U.; Liu, K.-Y.; Herbert, J. M. Accurate and efficient *ab initio* calculations for supramolecular complexes: Symmetry-adapted perturbation theory with many-body dispersion. *J. Phys. Chem. Lett.* **2019**, *10*, 2706–2714.
 - ⁷² Nguyen, B.; Chen, G. P.; Agee, M. M.; Burow, A. M.; Tang, M.; Furche, F. Divergence of many-body perturbation theory for noncovalent interactions of large molecules. *J. Chem. Theory Comput.* **2020**, *16*, 2258–2273.
 - ⁷³ Shee, J.; Loipersberger, M.; Hait, D.; Lee, J.; Head-Gordon, M. Revealing the nature of electron correlation in transition metal complexes with symmetry breaking and chemical intuition. *J. Chem. Phys.* **2021**, *154*, 194109:1–21.
 - ⁷⁴ Carter-Fenk, K.; Head-Gordon, M. Repartitioned Brillouin-Wigner perturbation theory with a size-consistent second-order correlation energy. *J. Chem. Phys.* **2023**, *158*, 234108:1–14.
 - ⁷⁵ Villot, C.; Ballesteros, F.; Wang, D.; Lao, K. U. Coupled cluster benchmarking of large noncovalent complexes in L7 and S12L as well as the C₆₀ dimer, DNA-ellipticine, and HIV-indinavir. *J. Phys. Chem. A* **2022**, *126*, 4326–4341.
 - ⁷⁶ Sedlak, R.; Janowski, T.; Pitoňák, M.; Řezáč, J.; Pulay, P.; Hobza, P. Accuracy of quantum chemical methods for large noncovalent complexes. *J. Chem. Theory Comput.* **2013**, *9*, 3364–3374.
 - ⁷⁷ Riplinger, C.; Sandhoefer, B.; Hansen, A.; Neese, F. Natural triple excitations in local coupled cluster calculations with pair natural orbitals. *J. Chem. Phys.* **2013**, *139*, 134101:1–13.
 - ⁷⁸ Riplinger, C.; Pinski, P.; Becker, U.; Valeev, E. F.; Neese, F. Sparse maps—A systematic infrastructure for reduced-scaling electronic structure methods. II. Linear scaling domain based pair natural orbital coupled cluster theory. *J. Chem. Phys.* **2016**, *144*, 024109:1–10.
 - ⁷⁹ Guo, Y.; Becker, U.; Neese, F. Comparison and combination of “direct” and fragment based local correlation methods: Cluster in molecules and domain based local pair natural orbital perturbation and coupled cluster theories. *J. Chem. Phys.* **2018**, *148*, 124117:1–11.
 - ⁸⁰ Prier, C. K.; Rankic, D. A.; MacMillan, D. W. C. Visible light photoredox catalysis with transition metal complexes: Applications in organic synthesis. *Chem. Rev.* **2013**, *113*, 5322–5363.
 - ⁸¹ Arias-Rotondo, D. M.; McCusker, J. K. The photophysics of photoredox catalysis: a roadmap for catalyst design. *Chem. Soc. Rev.* **2016**, *45*, 5803–5820.
 - ⁸² Förster, C.; Heinze, K. Photophysics and photochemistry with Earth-abundant metals – fundamentals and concepts. *Chem. Soc. Rev.* **2019**, *49*, 1057–1070.
 - ⁸³ Chan, A. Y.; Ghosh, A.; Yarranton, J. T.; Twilton, J.; Jin, J.; Arias-Rotondo, D. M.; Sakai, H. A.; McCusker, J. K.; MacMillan, D. W. C. Exploiting the Marcus inverted region for first-row transition metal-based photoredox catalysis. *Science* **2023**, *382*, 191–197.
 - ⁸⁴ Vériil, M.; Scemama, A.; Caffarel, M.; Lipparini, F.; Boggio-Pasqua, M.; Jacquemin, D.; Loos, P.-F. QUESTDB: A database of highly accurate excitation energies for the electronic structure community. *WIREs Comput. Mol. Sci.* **2021**, *11*, e1517:1–45.
 - ⁸⁵ Jacquemin, D.; Kossoski, F.; Gam, F.; Boggio-Pasqua, M.; Loos, P.-F. Reference vertical excitation energies for transition metal compounds. *J. Chem. Theory Comput.* **2023**, *19*, 8782–8800.
 - ⁸⁶ Radón, M.; Drabik, G.; Hodorowicz, M.; Szklarzewicz, J. Performance of quantum chemistry methods for a benchmark set of spin-state energetics derived from experimental data of 17 transition metal complexes (SSE17). *Chem. Sci.* **2024**, *15*, 20189–20204.
 - ⁸⁷ Yan, M.; Zhu, H.; Luo, H.; Zhang, T.; Sun, H.; Kannan, K. Daily exposure to environmental volatile organic compounds triggers oxidative damage: Evidence from a large-scale survey in China. *Environ. Sci. Technol.* **2023**, *57*, 20501–20509.
 - ⁸⁸ Zhou, X.; Zhou, X.; Wang, C.; Zhou, H. Environmental and human health impacts of volatile organic compounds: A perspective review. *Chemosphere* **2023**, *313*, 137489:1–

- 9.
- ⁸⁹ Mellouki, A.; Wallington, T. J.; Chen, J. Atmospheric Chemistry of Oxygenated Volatile Organic Compounds: Impacts on Air Quality and Climate. *Chem. Rev.* **2015**, *115*, 3984–4014.
- ⁹⁰ Li, Z. *et al.* Modeling the Formation of Organic Compounds across Full Volatility Ranges and Their Contribution to Nanoparticle Growth in a Polluted Atmosphere. *Environ. Sci. Technol.* **2024**, *58*, 1223–1235.
- ⁹¹ Huang, X. *et al.* Ozone Formation in a Representative Urban Environment: Model Discrepancies and Critical Roles of Oxygenated Volatile Organic Compounds. *Environ. Sci. Technol. Lett.* **2025**, *12*, 297–304.
- ⁹² Janoš, J.; Vinklárík, I. S.; Rakovský, J.; Mukhopadhyay, D. P.; Churchod, B. F. E.; Fárník, M.; Slavíček, P. On the wavelength-dependent photochemistry of the atmospheric molecule CF₃COCl. *ACS Earth Space Chem.* **2023**, *7*, 2275–2286.
- ⁹³ Thouless, D. J. Stability conditions and nuclear rotations in the Hartree-Fock theory. *Nucl. Phys.* **1960**, *21*, 225–232.
- ⁹⁴ Tuckman, H.; Neuscamman, E. Aufbau suppressed coupled cluster theory for electronically excited states. *J. Chem. Theory Comput.* **2024**, *20*, 2761–2773.
- ⁹⁵ III, G. D. P.; Sekino, H.; Bartlett, R. J. Multiplicity of many-body wavefunctions using unrestricted Hartree-Fock reference functions. *Collect. Czech. Chem. Commun.* **1988**, *53*, 2203–2213.
- ⁹⁶ Stanton, J. F. On the extent of spin contamination in open-shell coupled-cluster wave functions. *J. Chem. Phys.* **1994**, *101*, 371–374.
- ⁹⁷ Krylov, A. I. Spin-contamination of coupled-cluster wave functions. *J. Chem. Phys.* **2000**, *113*, 6052–6062.
- ⁹⁸ Schlegel, H. B. Møller-plesset perturbation theory with spin projection. *J. Phys. Chem.* **1988**, *92*, 3075–3078.
- ⁹⁹ Shiozaki, T.; Györfy, W.; Celani, P.; Werner, H.-J. Communication: Extended multi-state complete active space second-order perturbation theory: Energy and nuclear gradients. *J. Chem. Phys.* **2011**, *135*, 081106:1–4.
- ¹⁰⁰ Epifanovsky, E. *et al.* Software for the frontiers of quantum chemistry: An overview of developments in the Q-Chem 5 package. *J. Chem. Phys.* **2021**, *155*, 084801:1–59.
- ¹⁰¹ Neese, F.; Valeev, E. F. Revisiting the atomic natural orbital approach for basis sets: Robust systematic basis sets for explicitly correlated and conventional correlated *ab initio* methods? *J. Chem. Theory Comput.* **2011**, *7*, 33–43.
- ¹⁰² Sosa, C.; Geertsen, J.; Trucks, G. W.; Bartlett, R. J.; Franz, J. A. Selection of the reduced virtual space for correlated calculations. An application to the energy and dipole moment of H₂O. *Chem. Phys. Lett.* **1989**, *159*, 148–154.
- ¹⁰³ Taube, A. G.; Bartlett, R. J. Frozen natural orbitals: Systematic basis set truncation for coupled-cluster theory. *Collect. Czech. Chem. Commun.* **2005**, *70*, 837–850.
- ¹⁰⁴ Taube, A. G.; Bartlett, R. J. Frozen natural orbital coupled-cluster theory: Forces and application to decomposition of nitroethane. *J. Chem. Phys.* **2008**, *128*, 164101:1–17.
- ¹⁰⁵ III, A. E. D.; Sherrill, C. D. Accurate noncovalent interaction energies using truncated basis sets based on frozen natural orbitals. *J. Chem. Theory Comput.* **2013**, *9*, 293–299.
- ¹⁰⁶ Weigend, F.; Ahlrichs, R. Balanced basis sets of split valence, triple zeta valence and quadruple zeta valence quality for H to Rn: Design and assessment of accuracy. *Phys. Chem. Chem. Phys.* **2005**, *7*, 3297–3305.
- ¹⁰⁷ Rappoport, D.; Furche, F. Property-optimized Gaussian basis sets for molecular response calculations. *J. Chem. Phys.* **2010**, *133*, 134105:1–11.
- ¹⁰⁸ Gray, M.; Herbert, J. M. Comprehensive basis-set testing of extended symmetry-adapted perturbation theory and assessment of mixed-basis combinations to reduce cost. *J. Chem. Theory Comput.* **2022**, *18*, 2308–2330.
- ¹⁰⁹ Carter-Fenk, K.; Herbert, J. M. State-targeted energy projection: A simple and robust approach to orbital relaxation of non-Aufbau self-consistent field solutions. *J. Chem. Theory Comput.* **2020**, *16*, 5067–5082.
- ¹¹⁰ Gilbert, A. T. B.; Besley, N. A.; Gill, P. M. W. Self-consistent field calculations of excited states using the maximum overlap method (MOM). *J. Phys. Chem. A* **2008**, *112*, 13164–13171.
- ¹¹¹ Barca, G. M. J.; Gilbert, A. T. B.; Gill, P. M. W. Simple models for difficult electronic excitations. *J. Chem. Theory Comput.* **2018**, *14*, 1501–1509.

For table of contents only:

